Explicit approximations to estimate the perturbative diffusivity in the presence of convectivity and damping (Part 1): Semi-infinite slab approximations

M. van Berkel[1,2,3,4], H.J. Zwart[5,6], G.M.D. Hogeweij[3],
N. Tamura[1], S. Inagaki[7], M.R. de Baar[3,4], and K. Ida[1]

[1]*National Institute for Fusion Science,*
322 Oroshi-cho, Toki-city, Gifu, 509-5292, Japan

[2]*Fellow of the Japan Society for the Promotion of Science (JSPS)*

[3]*FOM Institute DIFFER-Dutch Institute for Fundamental Energy Research,*
Association EURATOM- FOM, Trilateral Euregio Cluster,
PO Box 1207, 3430 BE Nieuwegein, The Netherlands

[4]*Eindhoven University of Technology, Dept. of Mechanical Engineering,*
Control Systems Technology group, PO Box 513,
5600 MB Eindhoven, The Netherlands

[5]*Eindhoven University of Technology,*
Dept. of Mechanical Engineering, Dynamics and Control group,
PO Box 513, 5600 MB Eindhoven, The Netherlands

[6]*Department of Applied Mathematics,*
University of Twente, P.O. Box 217,
7500 AE Enschede, The Netherlands and

[7]*Research Institute for Applied Mechanics,*
Kyushu University, Kasuga 816-8580, Japan

Abstract

In this paper, a number of new approximations are introduced to estimate the perturbative diffusivity (χ), convectivity (V), and damping (τ) in cylindrical geometry. For this purpose the harmonic components of heat waves induced by localized deposition of modulated power are used. The approximations are based on semi-infinite slab approximations of the heat equation. The main result is the approximation of χ under the influence of V and τ based on the phase of two harmonics making the estimate less sensitive to calibration errors. To understand why the slab approximations can estimate χ well in cylindrical geometry, the relationships between heat transport models in slab and cylindrical geometry are studied. In addition, the relationship between amplitude and phase with respect to their derivatives, used to estimate χ, is discussed. The results are presented in terms of the relative error for the different derived approximations for different values of frequency, transport coefficients, and dimensionless radius. The approximations shows a significant region in which χ, V, and τ can be estimated well, but also regions in which the error is large. Also, it is shown that some compensation is necessary to estimate V and τ in a cylindrical geometry. On the other hand, errors resulting from the simplified assumptions are also discussed showing that estimating realistic values for V and τ based on infinite domains will be difficult in practice.

This paper is the first part (Part 1) of a series of three papers. In Part 2 and Part 3 cylindrical approximations based directly on semi-infinite cylindrical domain (outward propagating heat pulses) and inward propagating heat pulses in a cylindrical domain, respectively, will be treated.

I. GENERAL INTRODUCTION

The efficiency of future thermo-nuclear fusion reactors will be largely determined by the level of transport of heat and particles in the magnetically confined plasma. Magnetically confined plasmas are organized in nested surfaces of constant pressure and magnetic flux, which can be labeled by a dimensionless radius ρ, ranging from 0 at the magnetic axis to 1 at the last closed flux surface. The thermal transport is oriented perpendicular to these surfaces; consequently, thermal transport can be modeled in terms of a one-dimensional transport equation in ρ.

When one derives the diffusivity of a species j (χ_j) from the local power balance in steady state, the off-diagonal terms in the transport matrix, i.e., heat fluxes driven by, e.g., the density gradient and the temperature gradients of other species, contribute to the heat flux of species j. These contributions pollute the thus derived diffusivity, which is therefore usually called $\chi_\mathrm{j}^\mathrm{eff}$. An alternative and cleaner method to derive χ_j is to periodically perturb the plasma and describe the thermal transport as a linearized equation around steady state. This is the subject of this paper, which appears in three parts (Part 1, Part 2, and Part 3).

In this method, one analyzes heat pulses in the plasma induced by localized deposition of modulated power. The perturbed heat flux can be described by a linearized equation containing a diffusive, convectivity, and damping part, with an incremental diffusivity ($\chi_\mathrm{j}^\mathrm{inc}$), an effective convection speed V_j, and a damping term τ_j, respectively. The off-diagonal terms in the transport matrix act as a convectivity term; effects like the modulated electron-ion heat exchange and modulated ohmic heating are adequately captured in a damping term τ [1–3]. These parameters as function of ρ are called profiles. The heat pulse propagation and dispersion carry the information for the estimation of the profiles of $\chi_\mathrm{j}^\mathrm{inc}$, V_j and τ_j.

In this paper, various new approximations are presented for determining $\chi_\mathrm{j}^\mathrm{inc}$, V_j and τ_j. The quality of the individual approximations depend on ρ, the frequency ω, and the transport coefficients themselves. Hence, not only different approximations are necessary for different values of the transport coefficients, but also a selection method to select the proper approximation is necessary. Although the vast majority of perturbative transport studies so far were done for the electron channel, the methods described in this paper apply to any species j (electrons, ions, impurity species). In the remainder of the text we will drop the subscript "j" and the superscript "inc."

Perturbative analysis of thermal transport in magnetically confined plasmas started as early as in the 1970s, using heat waves that originated from the sawtooth instability [4, 5]. The first equations to analyze the perturbated transport were derived in this period, e.g., [6]. These were extended in the 1980s [7, 8] and the 1990s [9]. These equations use the harmonic components of the temperature perturbations at different radial locations to determine the perturbative thermal diffusion coefficient χ, which are now commonly used equations to analyze transport [1, 10–13]. They use the amplitude A and phase ϕ in terms of the spatial logarithmic amplitude derivative A'/A and spatial phase derivative ϕ'. However, these equations only approximate the thermal diffusion coefficient χ of the underlying cylindrical Partial Differential Equation (PDE) by either assuming a slab-geometry or by assuming ϕ' to be independent of ρ, i.e., $\phi'' = 0$, such that it can be used to derive a direct equation for χ. As such, these approximations do not approximate the thermal diffusion coefficient χ well in a plasma subject to strong cylindrical effects. In addition, the exact region in which χ is well approximated by these equations is not clear, which is caused by the fact that the quality of the approximation depends on the unknown χ to be estimated. Moreover, these equations only approximate the thermal diffusion coefficient and do not take the convectivity into account. The argument has been put forward that the convectivity and damping are negligible if a high enough modulation frequency is used. Although this argument is mathematically correct, at such high frequencies the heat waves will penetrate less deep, i.e., the amplitude of the perturbation will be smaller, whereas the noise level can be considered constant. Hence, measurements at these frequencies are more susceptible to noise, which leads to more uncertainty on the estimated diffusivity. Moreover, experiments are always performed at finite modulation frequencies such that the effect of convectivity and damping terms cannot be entirely excluded.

Working at low frequencies implies that in many cases the convectivity and the damping need to be taken into account. In addition, the increase in the size of fusion reactors and the corresponding increase in confinement time require a decrease in modulation frequencies at roughly the same rate. Decreasing the modulation frequencies also implies that the cylindrical effects become more dominant. Therefore, in this paper a large number of new approximations is derived, which estimate the diffusivity, the convectivity, and the damping in regions with strong cylindrical effects. These approximations can be used in any frequency range and as such χ, V, and τ can be estimated with much more precision than for

instance the method presented in [1, 14], where the limit of high frequency, resulting in noisy measurements, is necessary to determine χ first after which V and τ can be studied. In addition, these approximations also show a better performance in regimes with weak cylindrical effects (slab-like). More importantly, the quality of the approximations in relation to the original assumed model can be verified using the corresponding approximations of damping and possibly convectivity.

The new approximations still assume that the transport coefficients are independent of ρ and some still assume a semi-infinite domain. In addition, it is assumed that density gradients are negligible, which is one additional assumption compared to the cylindrical approximation derived in [9]. These assumptions simplify the problem significantly such that explicit approximations can be derived much more easily and still will allow for an approximation of the varying $\chi(\rho)$ profile. On the other hand, these assumptions introduce errors on the estimates, which need to be considered. For instance, these assumptions will limit the ability to estimate the convectivity and damping significantly. Nevertheless, including the damping and convectivity is important to arrive at better estimates of the diffusivity. To understand this, it is important to study and discuss these errors in detail, which requires an understanding of the original PDEs describing transport as introduced in [15–17]. As primarily the electron thermal diffusion coefficient is determined using the previously methods we limit ourselves to the discussion of the models related to the electron thermal transport.

This equation commonly used to describe the thermal transport does not address the underlying (turbulent) transport mechanisms directly, but rather tries to capture the effective thermal transport. Physics calculations suggest that the effective thermal transport is the result of the complex dynamics between streamers and zonal flows [1]. When zonal flows and drift-turbulence co-exist, the transport coefficients, e.g., χ (or heat-flux q) have a T, ∇T and k dependence, in which k is the inverse length scale of the turbulent fluctuations [11, 18, 19]. The k-space is an important tool to study the turbulent transport and the relationship between zonal flows and drift waves [18, 20, 21]. However, in this set of papers only the effective thermal transport is estimated (around an equilibrium) and not the underlying turbulent transport is estimated explicitly. In addition, the unnatural effect of the infinite domain boundary conditions and symmetry boundary conditions (finite domain) can have on the transport description in k-space domain related to the damping of the modes is not

discussed here (see [18]).

It is important to understand the underlying boundary conditions under which these approximations are derived. Therefore, not only the notion of the logarithmic temperature derivative is introduced, but also the notion of transfer functions is discussed to clarify the underlying assumptions and shed light on how A'/A and ϕ' are related to the measured amplitude A and ϕ. These transfer functions can also be used to test the quality of the approximation if other assumptions hold than under which these approximations have been derived.

The new approximations are based on the use of multiple harmonics, continued fractions, and asymptotic expansions. The multiple harmonics are necessary to determine the diffusivity, in the presence of convectivity and damping. On the other hand, it is well known that the solutions to the underlying cylindrical PDE can be expressed using higher transcendental functions [22], e.g., Bessel functions and Confluent Hypergeometric Functions. The ratio's of transcendental functions can often be well approximated by continued fractions [23, 24] and asymptotic expansions [25, 26].

There is a profound difference in cylindrical domains between heat waves traveling towards the edge (outward) or towards the plasma center (inward) in terms of their boundary conditions, thus also in terms of their solutions. Therefore, a clear distinction is made between inward and outward approximations. The outward approximations based on the semi-infinite domain include the cylindrical approximations derived in [7–9]. Interestingly, the phase only equation [5] and the cylindrical approximation [9] are also found as the simplest approximation using the technique of continued fractions.

In total more than 20 new approximations have been derived. The different approximations are compared for different values of ω, ρ, χ, V, and τ. It turns out that in the case $V = 0$ it suffices to combine two approximations for each case, i.e., one that estimates χ well in a strong cylindrical geometry and one in a weak cylindrical geometry (slab-like) to achieve small errors. However, to achieve the most accurate result a larger number of approximations are necessary. For the combined problem of the estimation of χ, V, and τ the new approximations show a significant region in which χ can be approximated well, but also regions in which no suitable approximation exists.

To increase the readability, this paper has been split into three parts. This part, Part 1, deals with semi-infinite slab approximations. Part 2 deals with semi-infinite (outward propa-

gating heat pulses) cylindrical approximations. Finally, Part 3 will deal with approximations for inward propagating heat pulses in cylindrical geometry.

II. INTRODUCTION TO PART 1

This paper, Part 1 of a series of three papers, deals with semi-infinite slab approximations. It is structured as follows. Section III gives an overview of the relevant models and simplifications of electron thermal transport in fusion reactors, which are necessary for the continuation of the paper. In Section IV the relationship between simplified models to determine the parameters, boundary conditions, and A'/A and ϕ' are explained; transfer functions, logarithmic temperature derivatives, and double spatial derivatives of A and ϕ are treated. Then, in Section V the concept of multiple harmonics is explored to determine new (and old) approximations to directly calculate the diffusivity, convectivity, and damping. In Section VI the explicit approximations derived so far are compared for different values of χ, V, and τ, and the selection of the best approximation is discussed. Then Section VII discusses the estimation of V and τ and common errors originating from infinite domain assumptions. Finally, in Section VIII the main results are summarized and discussed.

III. MODELING OF THERMAL TRANSPORT

In this section, the main assumptions and models used for perturbative transport analysis of the electron transport are summarized. In addition, it is shown that analyzing the thermal transport in slab-geometry allows for the determination of the diffusivity in cylindrical geometry.

A. Conservation of energy and particles

In this paper, only a periodically modulated electron heating source (P_{mod}) will be considered. Usually this will be modulated Electron Cyclotron Heating. However, any localized electron heating could be used, i.e Lower Hybrid Heating or Ion Cyclotron Heating in a suitable minority heating scheme. Therefore, it is reasonable to consider only the coupled

equations of particle density and electron heat transport defined in, e.g., [1, 15, 27, 28]:

$$\frac{\partial n}{\partial t} = -\nabla\Gamma + S_p, \tag{1}$$

$$\frac{\partial}{\partial t}\left(\frac{3}{2}nT\right) = -\nabla q + \nabla\left(\frac{5}{2}T\,\Gamma\right) + \frac{1}{n}\Gamma\nabla\left(nT\right) + S_h, \tag{2}$$

where q denotes the heat flux, Γ the particle flux, T the electron temperature, n the density, and S_p the particle sources. Based on [16] the source term S_h includes the electron-ion energy equipartition S_{ie}, the external heating power density S_f contributing to the energy balance, S_r the radiation losses due to Bremsstrahlung, S_{ohm} ohmic heating power, and P_{mod}. This leads to

$$S_h = S_f + S_{ohm} - S_r - S_{ie} + P_{mod}. \tag{3}$$

In this paper, it is assumed that all source terms except P_{mod} in S_h are static (do not depend on time) or their variation in time is assumed to be negligible compared to the perturbation induced by P_{mod}. Moreover, only perturbations of the thermal transport are considered, thus $\partial n/\partial t = 0$. The exact descriptions for the heat flux q and particle flux Γ are unknown. However, classically they are modeled by the laws of Fick [27]

$$\Gamma = -D\nabla n \tag{4}$$

and Fourier

$$q = -n\chi\nabla T. \tag{5}$$

Variations of these laws exist, for instance by considering a convective velocity term U in q [1], i.e.,

$$q = -n\chi\nabla T - nUT. \tag{6}$$

Based on these equations it is possible to derive a one-dimensional Partial Differential Equation (PDE), which can be used to identify the electron diffusivity χ.

B. Perturbative transport analysis

Generally thermal transport inside a fusion reactor is modeled as radial (1D) transport in a cylinder due to the magnetic confined plasma topology [1]. This allows for rewriting (2), using (6), in terms of partial derivatives with respect to ρ

$$\frac{\partial}{\partial t}\left(\frac{3}{2}nT\right) = \frac{1}{\rho}\frac{\partial}{\partial \rho}\left(\rho n\chi\frac{\partial T}{\partial \rho} + \rho nUT\right) + \frac{1}{\rho}\frac{\partial}{\partial \rho}\left(\rho\frac{5}{2}T\,\Gamma\right) + \frac{1}{n}\Gamma\frac{1}{\rho}\frac{\partial}{\partial \rho}\left(\rho nT\right) + S_h, \tag{7}$$

where the dependencies on the dimensionless radius ρ have been omitted. Although non-linear dependencies exist, e.g., T_e and ∇T, it is assumed that the temperature perturbation in S_h used to analyze the transport is small enough to assume linearity around the equilibrium temperature. In such cases the simplified PDEs given in (7) must be seen as the result of a linearization of transport equations [1]. In such a linearization, other effects can also be captured in the diffusivity, convectivity, and a damping term, e.g., the electron-ion heat exchange can be adequately captured in a damping term. In addition, non-linear dependencies of for instance χ on T and ∇T is then partly accounted for in the convective term and/or damping. Therefore, the one-dimensional parabolic PDE is generally expressed in a simplified form describing cylindrical geometry

$$\frac{\partial}{\partial t}\left(\frac{3}{2}nT\right) = \frac{1}{\rho}\frac{\partial}{\partial \rho}\left(\rho n\chi\left(\rho\right)\frac{\partial T}{\partial \rho} + \rho nV\left(\rho\right)T\right) - \frac{3}{2}n\tau_{inv}\left(\rho\right)T + S_h, \tag{8}$$

where $V = U + \frac{7}{2}\frac{\Gamma}{n}$ and $\tau_{inv} = \frac{2}{3}\frac{1}{n}\left(\Gamma' - \frac{n'}{n}\Gamma\right)$ denote the convectivity and damping in cylindrical geometry based on (7) only. The damping is denoted by its inverse, i.e., $\tau_{inv} \equiv \tau^{-1}$ and the prime, in e.g., n', denotes the spatial derivative with respect to ρ. The reason for this change of variables is that τ_{inv} is bounded making it easier to represent in plots. In addition, it also is easily transformed back to the well known damping $\tau = 1/\tau_{inv}$. However, if τ is needed it can simply be calculated $\tau = 1/\tau_{inv}$. The diffusivity $\chi\left(\rho\right)$, the (effective) convectivity $V\left(\rho\right)$, and the (inverse) damping $\tau_{inv}\left(\rho\right)$ in front of T, T', and T'' can be identified by only considering electron temperature perturbations.

Unfortunately, (8) is difficult to use in practice to estimate χ from measurements. Therefore, a number of simplification steps are applied [9]. Only measurements are considered for which the transients due to the initial condition can be neglected. It is assumed that the parameters are constant with respect to time and ρ. Thus the parameters are assumed to be homogenous or uniform [1, 9]. In addition, only spatial regions are considered where $P_{mod} = 0$, i.e., outside the region where the heating is deposited to perturb the plasma such

that (8) is simplified to

$$\frac{\partial}{\partial t}\left(\frac{3}{2}nT\right) = \frac{1}{\rho}\frac{\partial}{\partial \rho}\left(\rho n\chi\frac{\partial T}{\partial \rho} + \rho nVT\right) - \frac{3}{2}n\tau_{inv}T. \tag{9}$$

This equation is often used in the literature [1, 9] to analyze heat wave propagation in a cylindrical geometry. Alternatively, for large ρ the slab geometry representation of (9) is used to analyze transport in a cylindrical geometry [1, 7, 9].

C. Slab geometry representation and its relationship to cylindrical geometry

In slab-geometry the following representation is used to determine χ explicitly [1]

$$\frac{3}{2}\frac{\partial T}{\partial t} = \chi\frac{\partial^2 T}{\partial \rho^2} + V_s\frac{\partial T}{\partial \rho} - \frac{3}{2}\tau_{invs}T, \tag{10}$$

where χ, V_s, and τ_{invs} are independent of ρ.

It is important to realize that the effective convectivity $V \neq V_s$ and the inverse damping $\tau_{inv} \neq \tau_{invs}$ represent something different in (10) and (9). This can be investigated by transforming (9) assuming $n' = 0$:

$$\frac{\partial}{\partial t}\left(\frac{3}{2}T\right) = \chi\frac{\partial^2 T}{\partial \rho^2} + \left(V + \frac{\chi}{\rho}\right)\frac{\partial T}{\partial \rho} - \frac{3}{2}\left(\tau_{inv} - \frac{2}{3}\frac{V}{\rho}\right)T. \tag{11}$$

This means that only when $\rho \to \infty$, $V = V_s$ and $\tau_{inv} = \tau_{invs}$. Hence, (10) will be a proper approximation of (9) when n' is negligible and the variations χ/ρ and V/ρ are small with respect to V and τ_{inv}, respectively. The diffusivity term χ in front of T'' is unaffected by this change of geometry. On the other hand, the diffusivity term in cylindrical geometry now also appears as a pseudo convectivity χ/ρ in slab geometry. The pseudo convectivity also points out a simple problem regarding the comparison of the power balance diffusivity χ^{PB} as defined in [1]

$$\chi^{PB} = -\frac{q}{n\nabla T} \tag{12}$$

and the heat pulse diffusivity χ in cylindrical geometry, which is often denoted as χ^{HP}. The power balance (12) is generally analyzed in slab-geometry such that the term χ/ρ is

not taken into account. This already results in $\chi^{PB} \neq \chi^{HP}$. Therefore, χ^{PB} will not be considered in this paper.

In the next section, based on (10) direct expressions for χ are derived to analyze the transport coefficients in a cylindrical geometry.

IV. SIMPLIFIED MODELS FOR DESCRIBING THERMAL TRANSPORT

In this section the classic relationships to determine χ are derived. Therefore, the Laplace transform of (10) is used

$$\frac{3}{2}s\Theta = \chi \frac{d^2\Theta}{d\rho^2} + V_s \frac{d\Theta}{d\rho} - \frac{3}{2}\tau_{invs}\,\Theta, \tag{13}$$

where s is the Laplace variable and $\Theta(\rho, s)$ is the Laplace transform of $T(\rho, t)$ [29]. The Laplace variable can in practice only be measured on the imaginary axis, thus $s = i\omega$. The general solution of (13) is given by [30]

$$\begin{aligned} \Theta(\rho, s) &= C_1(s)\exp(\lambda_1\rho) + C_2(s)\exp(\lambda_2\rho) \\ \text{with} \qquad \lambda_{1,2} &= -\frac{V_s}{2\chi} \mp \sqrt{\left(\frac{V_s}{2\chi}\right)^2 + \frac{3}{2}\frac{s+\tau_{invs}}{\chi}}. \end{aligned} \tag{14}$$

The boundary constants $C_1(s)$ and $C_2(s)$, which are independent of ρ, are determined by the choice of the boundary conditions.

There are basically three approaches to derive approximations for χ, which distinguish themselves by the choice for $C_1(\omega)$ and $C_2(\omega)$ in (14): 1) transfer functions, in which both $C_1(s)$ and $C_2(s)$ are fixed explicitly; 2) the logarithmic temperature derivative, i.e., $(\partial\Theta/\partial\rho)/\Theta$, in which only one boundary constant is fixed explicitly by introducing the spatial logarithmic derivative of the amplitude A and the spatial derivative of ϕ; 3) An approach in which fixing $C_1(s)$ and $C_2(s)$ are avoided by introducing double spatial derivatives to A and ϕ. However, as a solution of a second order PDE is only defined by two boundary conditions; there must be a clear relationship between these three approaches. This is derived in this section giving insight in how A and ϕ are related to their spatial derivatives.

A. Description between measurements: transfer function

The transfer function approach may be less familiar in the fusion literature [31–33], but it is extensively used in the field of system identification [34, 35]. From the available

fusion literature on transfer functions it may seem that only rational functions based on measurement data are applicable. However, as will be shown here, transfer functions can also be used to describe simplified models for PDEs [36], which are of non-rational form.

The most important advantage of this technique over the other two techniques is that it only depends on the measurements. Hence, it is no longer required to approximate the spatial derivative of phase ϕ and the spatial logarithmic amplitude derivative of A. The derivation will be performed for heat waves traveling towards the edge (outwards).

The first boundary constant $C_2(s)$ will be fixed by assuming an infinite domain. This choice is commonly used [1, 9] as it simplifies the solution significantly such that approximations for χ can be easily derived.

The infinite domain boundary condition is defined as follows, if $\rho \to \infty$, then $\Theta \to 0$. This means that at $\rho = \infty$ all perturbations need to have vanished. Since, we follow the standard convention that for $z \in \mathbb{C}$, $\arg(z) \in (-\pi, \pi]$ and $\arg(\sqrt{z}) = \frac{1}{2}\arg(z)$, the two eigenfunctions in (14) satisfy $\exp(\lambda_1 \rho) \to 0$ and $|\exp(\lambda_2 \rho)| \to \infty$ for $\rho \to \infty$. Hence, $C_2(s) = 0$, otherwise the solution (14) would not converge to zero at large ρ. Then, the solution (14) is simplified to

$$\Theta(\rho, s) = C_1(s) \exp(\lambda_1 \rho). \tag{15}$$

The other boundary condition is chosen to be the temperature at the spatial location ρ_1, i.e., $\Theta(\rho, s) = \Theta(\rho_1, s)$, which in contrast to the assumption of an infinite boundary condition is only a weak assumption. The domain on which the transport coefficients are estimated cannot contain a source term. However, this domain should still be limited by some boundary condition. Hence, $\Theta(\rho_1, s)$ is used, which is a measured quantity. The boundary constant is then given by

$$C_1(s) = \exp(-\lambda_1 \rho_1)\, \Theta(\rho_1, s). \tag{16}$$

This determines the solution of (14), $\Theta(\rho, s)$, such that

$$\Theta(\rho, s) = \exp(\lambda_1 (\rho - \rho_1))\, \Theta(\rho_1, s). \tag{17}$$

The solution at a second measurement point $\rho_2 > \rho_1$ is denoted by $\Theta(\rho_2)$. Then (17) can be re-expressed as

$$\frac{\Theta(\rho_2, s)}{\Theta(\rho_1, s)} = \exp(\lambda_1 (\rho_2 - \rho_1)). \tag{18}$$

The left hand-side is built from the measured complex valued Fourier coefficients at measurement locations ρ_1 and ρ_2. On the right hand side are the unknown parameters contained

in λ_1. After the transport coefficients χ, V, and τ_{inv} have been determined, the transport coefficients can be substituted in (18). Then the right hand side can be directly compared to the measured left hand side to determine the quality of the estimated parameters. Similarly, the transfer functions for a cylindrical domain can be derived. In practice, the Laplace variable s can only be measured on the imaginary axis such that $s = i\omega$.

A simplified case of (18) in which $V = 0$ and only one harmonic is used i.e., $s = i\omega$ is fixed. Thus, the temperatures at fixed ω at two spatial locations can be expressed as $\Theta(\rho_1) = A_1 e^{i\phi_1}$ and $\Theta(\rho_2) = A_2 e^{i\phi_2}$ such that the transfer function (18) can be rewritten as

$$\frac{A_2 e^{i\phi_2}}{A_1 e^{i\phi_1}} = \exp\left(\sqrt{\frac{3}{2}\frac{i\omega + \tau_{invs}}{\chi}}\Delta\rho\right), \tag{19}$$

where $\Delta\rho = \rho_2 - \rho_1$. Applying the natural logarithm and taking the square of (19) results in

$$\ln\left(\frac{A_2}{A_1}\right)^2 - (\phi_2 - \phi_1)^2 + 2\ln\left(\frac{A_2}{A_1}\right) i(\phi_2 - \phi_1) = \frac{3}{2}\frac{i\omega + \tau_{invs}}{\chi}\Delta\rho^2. \tag{20}$$

The diffusivity χ can only be calculated properly if the phase is unwrapped, which means that possible additional 2π rotations between ρ_2 and ρ_1 need to be accounted for. Now by considering the imaginary part of (20), χ can be determined

$$\chi_{s4} = \frac{3}{4}\frac{\omega}{\frac{\ln(A_2)-\ln(A_1)}{\Delta\rho}\left(\frac{\phi_2-\phi_1}{\Delta\rho}\right)}. \tag{21}$$

The notation χ_{s4} is used instead of χ, to distinguish this specific form of χ as in this paper many other approximations are found to calculate χ. The damping τ_{invs} can also be calculated by considering the real part

$$\tau_{s4} = \frac{\omega}{2}\left(\frac{\ln(A_2) - \ln(A_1)}{\phi_2 - \phi_1} - \frac{\phi_2 - \phi_1}{\ln(A_2) - \ln(A_1)}\right). \tag{22}$$

It is clear that two measurement points suffice to determine χ using slab-geometry, in the presence of damping and under the assumption that the transport coefficients are independent of ρ. This description does not require any approximation of the derivatives A' and ϕ' as is used in [9].

B. Logarithmic temperature derivative

The logarithmic temperature derivative is defined as the ratio of the spatial derivative of the temperature and the temperature (in the frequency domain), i.e., $\Theta'(\rho)/\Theta(\rho)$. This means only one boundary condition is necessary. The other boundary condition is implicitly contained in the resulting A' and ϕ'. The solution needs to be simplified to find an explicit equation for χ and so again a semi-infinite slab-geometry is chosen, i.e., $C_2 = 0$ in (14). Taking the spatial derivative of $\Theta(\rho)$ results in

$$\frac{\partial\Theta(\rho)}{\partial\rho} = C_1(s)\,\lambda_1 \exp(\lambda_1\rho), \tag{23}$$

such that

$$\frac{\Theta'}{\Theta} = \lambda_1. \tag{24}$$

The temperature is written again in terms of its harmonic components, i.e., $\Theta = A\exp(i\phi)$ and $\Theta' = A'\exp(i\phi) + i\phi' A\exp(i\phi)$ such that the left hand side of (24) becomes

$$\frac{A'}{A} + i\phi' = \frac{\Theta'}{\Theta}, \tag{25}$$

which is independent of the chosen geometry such that it also holds in cylindrical geometry. Substituting (25) into (24) and taking the spatial derivative results in

$$\frac{d}{d\rho}\left(\frac{A'}{A}\right) + i\phi'' = 0. \tag{26}$$

Hence, the second spatial logarithmic derivative $d(A'/A)/d\rho = 0$ and the second spatial derivative $\phi'' = 0$ even in the presence of V, because λ_1 is independent of ρ. This means that in slab-geometry the spatial derivatives always satisfy

$$\frac{A'}{A} = \frac{d}{d\rho}(\ln(A)) \equiv \frac{\ln(A_2/A_1)}{\Delta\rho},\ \phi' \equiv \frac{\phi_2 - \phi_1}{\Delta\rho}. \tag{27}$$

This also follows directly from the transfer function description. This is shown by squaring (25) and if again it is assumed that $V = 0$, the right-hand side is exactly the same as the right hand side in (20)

$$\left(\frac{A'}{A}\right)^2 + 2\frac{A'}{A}\phi' i - (\phi')^2 = \frac{3}{2}\frac{\omega i + \tau_{invs}}{\chi}. \tag{28}$$

The left-hand side can be made explicit by introducing a boundary condition. In case $\Theta(\rho, s) = \Theta(\rho_1, s)$ is used the left-hand side of (28) needs to equal the left-hand side of

(20). This results in A'/A and ϕ' in slab-geometry to be defined as (27), which also shows the equivalence of the transfer function representation and the logarithmic temperature derivative.

When $\tau_{inv} = 0$, (20) or (28) can be expressed in terms of the amplitude and phase measurements at two locations [5–9]

$$\chi_{s1} = \frac{3}{4}\frac{\omega}{(\phi')^2}, \tag{29}$$

$$\chi_{s2} = \frac{3}{4}\frac{\omega}{(A'/A)^2}, \tag{30}$$

and

$$\chi_{s3} = \frac{3\omega}{(A'/A + \phi')^2}, \tag{31}$$

where ϕ' and A'/A are given according to (27). From a mathematical point of view: if an assumption is made on the parameter dependence (here that the transport coefficients are independent of ρ) and boundary conditions, then the properties of the spatial derivatives A' and ϕ' follows automatically as is shown here. On the other hand, if one makes a choice for the approximation of the derivatives, then automatically one has assumed a certain spatial dependence on the parameters and boundary condition. As such, fitting ϕ' and A' differently from (27) is a direct violation of the assumption that the parameters are independent of ρ. On the other hand, if more complicated relationships are used, e.g., cylindrical geometry, the derivatives A'/A and ϕ' are not so easily expressed in terms of A_2, A_1, ϕ_1, and ϕ_2.

C. Double spatial derivatives of A and ϕ

It is also possible to use only spatial derivatives of A and ϕ. As a second order PDE is used, these relationships include the double spatial derivatives A'' and ϕ''. This approximation is found by substituting $\Theta = A\exp(i\phi)$, $\Theta' = A'\exp(i\phi) + i\phi' A\exp(i\phi)$, and $\Theta'' = A''\exp(i\phi) + i\phi' A'\exp(i\phi) + iA'\phi'\exp(i\phi) - (\phi')^2 A\exp(i\phi) + iA\phi''\exp(i\phi)$ in (13) and by dividing by $A\exp(i\phi)$.

In slab-geometry this is not so useful as it has already been shown in (26) that ϕ'' and $\frac{d}{d\rho}\left(\frac{A'}{A}\right)$ equal zero. However, by expressing (13) in terms of double spatial derivatives it is easily shown that the three approaches are equivalent and that the boundary conditions and spatial dependencies are again contained within the spatial derivatives.

In cylindrical geometry (7) also Θ' and Θ'' can be substituted resulting in (for the imaginary part) [9]

$$\chi(\rho) = \frac{1.5\omega - \left(2.5\frac{\Gamma}{n} + \Gamma\right)\phi'}{\phi'' + \left(2\frac{A'}{A} + \frac{1}{\rho} + \frac{n'}{n} + \frac{\chi'}{\chi} + \frac{U(\rho)}{\chi}\right)\phi'} \tag{32}$$

for completeness also Γ and n (which are assumed constant in this paper) are included. In this representation Γ and n and its gradient n' can be included. On the other hand, (32) is only feasible in practice by assuming χ to be constant such that $\chi'/\chi = 0$ and assuming the convectivity zero, i.e., $U(\rho) = 0$. More importantly, the double derivatives will be extremely difficult to approximate in practice due to noise and the spacing between measurement channels. Therefore, ϕ'' is assumed to be zero in [9], and χ can be calculated using the simplified form of (32), i.e.

$$\chi_c = \frac{1.5\omega}{(2A'/A + 1/\rho + n'/n)\,\phi'}. \tag{33}$$

The assumption of $\phi'' = 0$ basically means that (33) is not a true cylindrical approximation as ϕ'' is not zero under the influence of cylindrical geometry. The advantage of χ_c compared to the rest of the approximations derived in this paper is that it can include density gradients, which are assumed constant in this paper ($n' = 0$).

V. DERIVATION OF EXPLICIT APPROXIMATIONS

Here, a new approximation for determining the χ, V, and τ_{inv} is introduced based on the use of two harmonics. The approximation is based on slab-geometry. However, including the convectivity in slab geometry allows for a partial compensation of the pseudo convectivity χ/ρ introduced when transforming cylindrical geometry into slab geometry in (11) making it more applicable to estimate χ in cylindrical geometry.

Every harmonic fixes two degrees of freedom, which means in practice that either χ and τ_{inv} or χ and V can be estimated if only one harmonic is used. Therefore, to estimate χ, V and τ_{inv} together, it is necessary to use at least two harmonics. This is easily understood if the solution is derived. Therefore, consider the semi-infinite slab-geometry solution again (repeated equation, hence same number)

$$\frac{\Theta'}{\Theta} = \lambda_1. \tag{24}$$

The principal square root in λ_1 can be split in its real and imaginary part using

$$\lambda_1 = -\frac{V_s}{2\chi} - (\alpha + \beta i) \tag{34}$$

where

$$(\alpha + \beta i)^2 = \left(\frac{V_s}{2\chi}\right)^2 + \frac{3}{2}\frac{(\tau_{invs} + i\omega)}{\chi}, \tag{35}$$

Hence,

$$\alpha^2 - \beta^2 = \left(\frac{V_s}{2\chi}\right)^2 + \frac{3}{2}\frac{\tau_{invs}}{\chi} \tag{36}$$

and

$$2\alpha\beta = \frac{3}{2}\frac{\omega}{\chi}. \tag{37}$$

The coefficients α and β can also be used to express A'/A and ϕ' defined according to (27), by taking the real and imaginary part of λ_1 using (24), (34), and (25), i.e.

$$\frac{A'}{A} = -\left(\frac{V_s}{2\chi} + \alpha\right) \qquad \phi' = -\beta. \tag{38}$$

The constants α and β are determined by rewriting (36) and (37)

$$4\chi^2\alpha^4 - \left(V_s^2 + 6\chi\tau_{invs}\right)\alpha^2 = \frac{9}{4}\omega^2, \tag{39}$$

$$4\chi^2\beta^4 + \left(V_s^2 + 6\chi\tau_{invs}\right)\beta^2 = \frac{9}{4}\omega^2. \tag{40}$$

Both (39) and (40) are fourth order equations yielding four solutions for α and four for β. Fortunately, not all of these solutions are feasible, because under natural assumptions $\omega > 0$ and $\chi > 0$ and a semi-infinite domain, ϕ' is negative. This means that according to (38), $\beta > 0$. In addition, following the definition in (37) the product of α and β is always positive, hence $\alpha > 0$.

There are three degrees of freedom (unknowns) in (35), which means that at least two harmonics ω_1 and ω_2 must be used. Consequently, one derivative is unnecessary, e.g., $\phi'(\omega_1)$ or $A'(\omega_2)/A(\omega_2)$. However, χ can be determined by only using $\phi'(\omega_1)$ and $\phi'(\omega_2)$, because (40) only contains two unknowns χ and $C_V = (V_s^2 + 6\chi\tau_{invs})$ such that

$$\chi_\phi = \frac{3}{4}\sqrt{\frac{\left(\omega_1\phi'_{\omega_2}\right)^2 - \left(\omega_2\phi'_{\omega_1}\right)^2}{\phi'^2_{\omega_1}\phi'^2_{\omega_2}\left(\phi'^2_{\omega_1} - \phi'^2_{\omega_2}\right)}}, \tag{41}$$

using the notations $\phi'_{\omega_1} = \phi'(\omega_1)$ and $\phi'_{\omega_2} = \phi'(\omega_1)$. The definition of the spatial phase derivatives in (41) is given by (27). This formula is based on the phase only, hence insensitive

to calibration errors. However, useful amplitude information is ignored, which can reduce the accuracy of the estimate significantly. The convectivity V_s is found by solving for α in (39) and substituting it into (38) such that

$$V_\phi = -2\chi_\phi \frac{A'}{A} - \sqrt{\frac{C_V + \sqrt{C_V^2 + 36\chi_\phi^2\omega^2}}{2}}, \tag{42}$$

where C_V is found by solving (40)

$$C_V = \frac{9}{4}\omega^2 \left(\phi'\right)^{-2} - 4\chi_\phi^2 \left(\phi'\right)^2. \tag{43}$$

The damping τ_{invs} is calculated from C_V

$$\tau_\phi = \frac{C_V - V_\phi^2}{6\chi_\phi}. \tag{44}$$

It is not possible to calculate the convectivity or damping from the phase only, unless either the damping or convectivity is considered negligible. In the noiseless slab-geometry case, it does not matter if ω_1 or ω_2 is used for ω in $\frac{A'}{A}$ and ϕ'. However, in practice generally the best choice is to use a weighted average as described in [37]. Easier to implement, but less accurate is to use ω_1 as it has generally the best Signal-to-Noise ratio (SNR). This also means that the second harmonic is generally more sensitive to noise, which can introduce an error and reduce the accuracy. On the other hand, by designing proper modulation signals this effect can be minimized. This is typically done by choosing a duty cycle different from 50% such that a similar first and second harmonic is created with similar SNRs, e.g., [38]. In addition, as convectivity and damping is included in this approximation it is no longer necessary to work in the limit of high frequency allowing lower excitation frequencies to be used with a better SNR. Here, only one variation has been given to calculate χ, V_s, and τ_{invs} using mainly the phase. There exists a number of variations using also $A'(\omega_1)/A(\omega_1)$ and $A'(\omega_2)/A(\omega_2)$.

In the special case that τ_{invs} is considered to be zero a single harmonic suffices to estimate both χ and V_s. This can be derived from (36) and (37), which results in

$$\chi_V = \frac{3}{2}\frac{\omega\frac{A'}{A}}{\left(\left(\frac{A'}{A}\right)^2 + \left(\phi'\right)^2\right)\phi'} \tag{45}$$

and

$$V_V = \frac{3}{2}\frac{\omega\left(\left(\phi'\right)^2 - \left(\frac{A'}{A}\right)^2\right)}{\left(\left(\frac{A'}{A}\right)^2 + \left(\phi'\right)^2\right)\phi'}. \tag{46}$$

These approximations together with the well known equations in the literature will be used to approximate χ, V, and τ_{inv} in cylindrical geometry.

VI. ESTIMATING χ UNDER INFLUENCE OF V AND τ_{inv}

In this section, the explicit approximations for χ, i.e., (29), (30), (31), (21), (41), and (33) are compared for different values of ρ, ω, χ, V, and τ_{inv}. For the comparison the true values of A'/A and ϕ' in a semi-infinite cylindrical geometry are used based on heat waves traveling outwards (away from the center). These are generated using the analytical solution of (9), which has been validated using a finite difference simulation of (9) with $\Theta(\rho \gg 1) = 0$.

It is cumbersome to make a comparison for five parameters (ρ, ω, χ, V, and τ_{inv}). However, it is possible to reduce this to four parameters by normalizing the transport coefficients with ω, e.g., (13) with $s = i\omega$ can be re-expressed as

$$\frac{3}{2} i\Theta = \frac{\chi}{\omega} \frac{d^2\Theta}{d\rho^2} + \frac{V_s}{\omega} \frac{d\Theta}{d\rho} - \frac{3}{2} \frac{\tau_{invs}}{\omega} \Theta. \tag{47}$$

This can also be done exactly the same in cylindrical geometry. In case two harmonics are necessary, $\phi'(\omega_1)$ and $\phi'(\omega_2)$ are calculated using $\omega_1 = \omega$ and $\omega_2 = 2\omega$ corresponding to the first and second harmonic. Consequently, the normalized transport coefficients in a cylindrical geometry are given by $\bar{\chi} = \chi/\omega$, $\bar{V} = V/\omega$, and $\bar{\tau}_{inv} = \tau_{inv}/\omega$ such that the heat equation and its solutions no longer depend ω explicitly.

This section consists of three parts: a presentation and discussion on the selection of the best approximations when only χ is considered; a similar discussion when χ and τ_{inv} are considered ($V = 0$); and when χ, V, and τ_{inv} are considered.

A. Diffusivity only

The comparison for χ only ($V = 0$ and $\tau_{inv} = 0$) is made based on a large number of possibilities of χ, ω, and ρ in terms of the normalized $\bar{\chi}$. The approximations are shown in Fig. 1 in terms of the relative error with respect to the true diffusivity χ.

It is clear that all approximations perform well in a slab-like geometry such that they approximate χ well if the ratio $\rho/\bar{\chi}$ is large. In χ_c large relative errors are observed for small $\rho/\bar{\chi}$, which can be understood by considering χ_c in (33). The large error is caused by ρ^{-1}

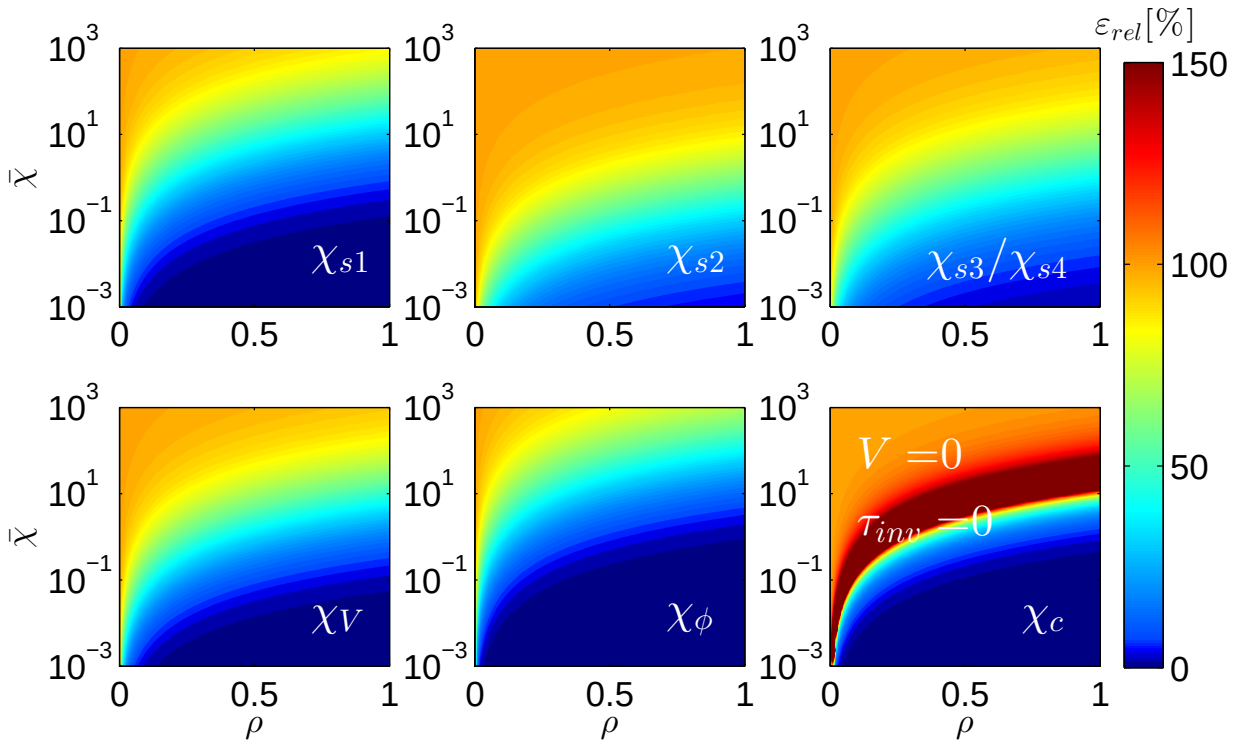

Figure 1: Comparison between the different relative errors of the χ estimates for a large range of $\bar{\chi} = \chi/\omega$ and ρ. The relative error is defined as $\varepsilon_{rel} = 100 \times \frac{|\chi - \chi_{est}|}{\chi}$ [%], where χ_{est} is one of the possible approximations. Note, that $V = \tau_{inv} = 0$ is the same as $\bar{V} = \bar{\tau}_{inv} = 0$. In this case χ_{s3} and χ_{s4} were almost exactly the same in terms of their error. This comparison is based on a cylindrical geometry using an infinite domain boundary condition assuming χ independent of ρ and $V = \tau_{inv} = 0$, where the heat waves travel outwards. The darkest blue represents $\varepsilon_{rel} < 1\%$ and the darkest red represents all $\varepsilon_{rel} > 150\%$.

term in χ_c, which over compensates resulting in a higher estimated diffusivity [9]. The A'/A and ϕ' are negative quantities for heat waves traveling outwards. Hence, the sum of ρ^{-1} and A'/A results in zero at the center of the dark red area. On the other hand, it is also clear that compared to the other slab-geometry approximations χ_c and χ_ϕ perform better. The approximation χ_ϕ is more accurate in a slightly larger region then the approximation χ_c. However, it is also important to note again that χ_ϕ is based on the phase of two harmonics instead of amplitude and phase of one harmonic as is the case for χ_c making it less comparable.

B. Diffusivity and damping

Only three approximations are available to estimate χ under the influence of damping τ_{inv}, i.e., χ_{s4} in (21), χ_ϕ in (41), and χ_c in (33). The approximations are presented at a limited number of spatial locations ρ. In order to have significant impact on the heat pulse propagation, τ should be of the order of the energy confinement time (τ_e), i.e., 1 s for JET or ITER. Therefore, the range of τ is chosen such that $0.5 < \tau < \infty$ ($\tau = \infty$ meaning no damping), i.e., $0 \leqslant \tau_{inv} \leqslant 2$. This range is the same for the normalized $\bar{\tau}_{inv}$ as the applicable range of ω is assumed $\omega > 1$ [rad/s].

In general the effect of damping τ_{inv} is not directly influenced by the cylindrical geometry ($V = 0$), which can be understood by comparing (10) and (11). In addition, τ_{inv} acts as a shift parameter in (10), which basically shifts the solution in ρ. This means that for large τ_{inv} the regions in which χ are approximated well is extended for increasing τ_{inv}. However, these effects are also influenced by the approximation error in χ and V. Therefore, it is not a one-to-one relationship. This can also be seen in Fig. 2, where with increasing τ_{inv} also the approximation region increases for all approximations.

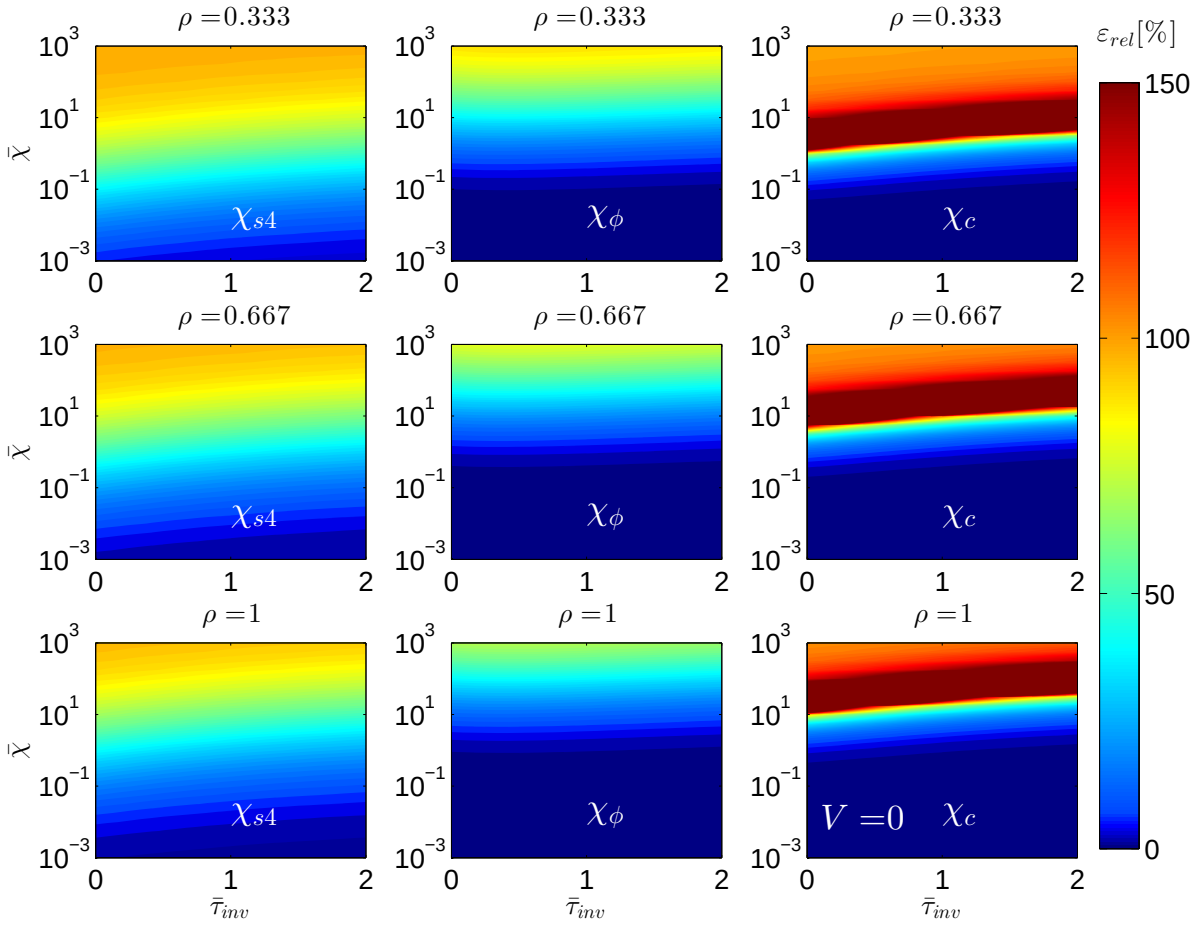

Figure 2: Comparison between the relative errors of the χ estimates using χ_{s4}, χ_ϕ, and χ_c for a large range of $\bar{\chi} = \chi/\omega$, $\bar{\tau}_{inv}$ and ρ. This comparison is based on a cylindrical geometry using an infinite domain boundary condition assuming constant spatial dependencies of χ and τ_{inv}. The darkest blue represents $\varepsilon_{rel} < 1\%$ and the darkest red represents all $\varepsilon_{rel} > 150\%$.

All approximations under the influence of damping behave similar to the case of χ only.

C. Diffusivity, convectivity, and damping

If χ, V, and τ_{inv} need to be estimated at least two harmonics are necessary. This also means that it is no longer possible to estimate χ with χ_c as is illustrated in Fig. 3, which is also well known in the literature [9].

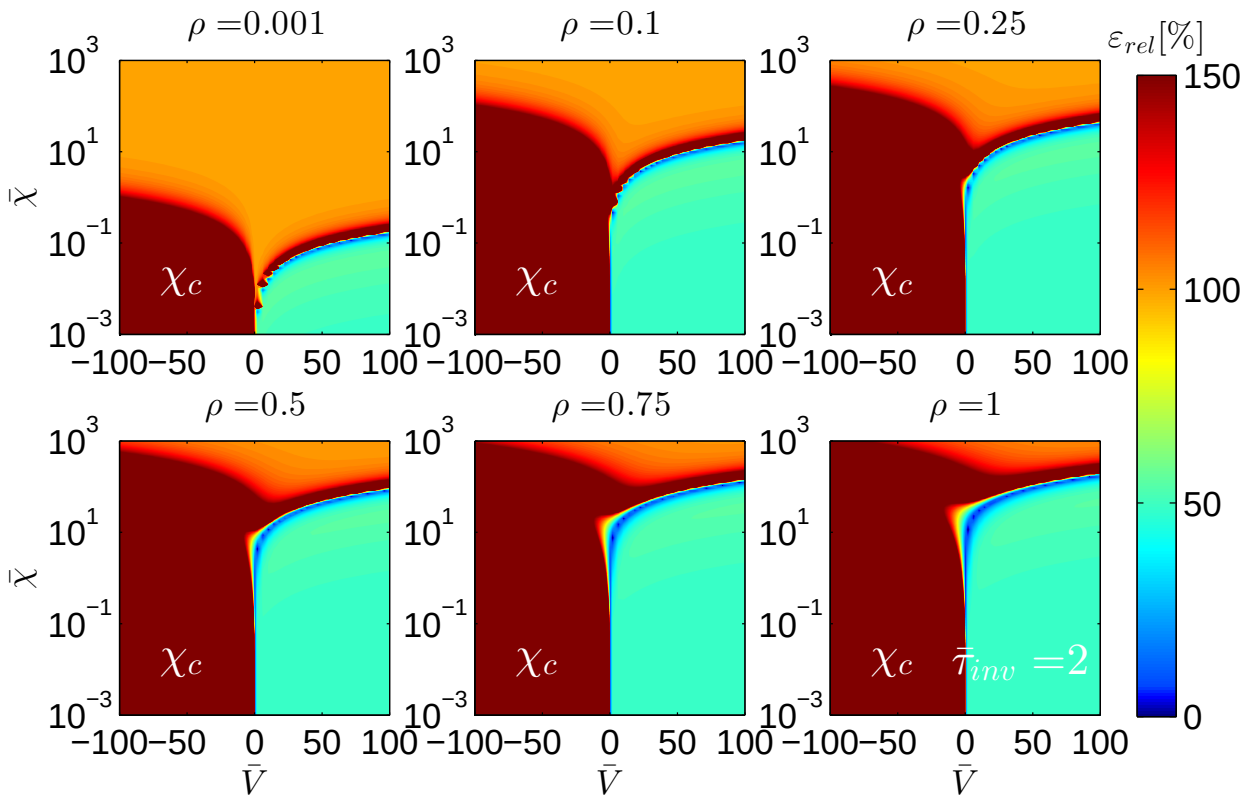

Figure 3: The relative errors of the χ_c estimates as function of $\bar{\chi} = \chi/\omega$, V and ρ. These errors are based on a cylindrical geometry using an infinite domain boundary condition where χ, V, and $\tau_{inv} = 2$ are independent of ρ. The heat waves travel outwards. The darkest blue represents $\varepsilon_{rel} < 1\%$ and the darkest red represents all $\varepsilon_{rel} > 150\%$.

On the other hand, χ can be estimated using χ_ϕ for a large range of parameters as is shown in Fig. 4. It is unclear what a good range is for the parameter $\bar{V} = V/\omega$ except that it can also be negative. Therefore, an arbitrary choice for this range is made $-100 \leqslant \bar{V} \leqslant 100$.

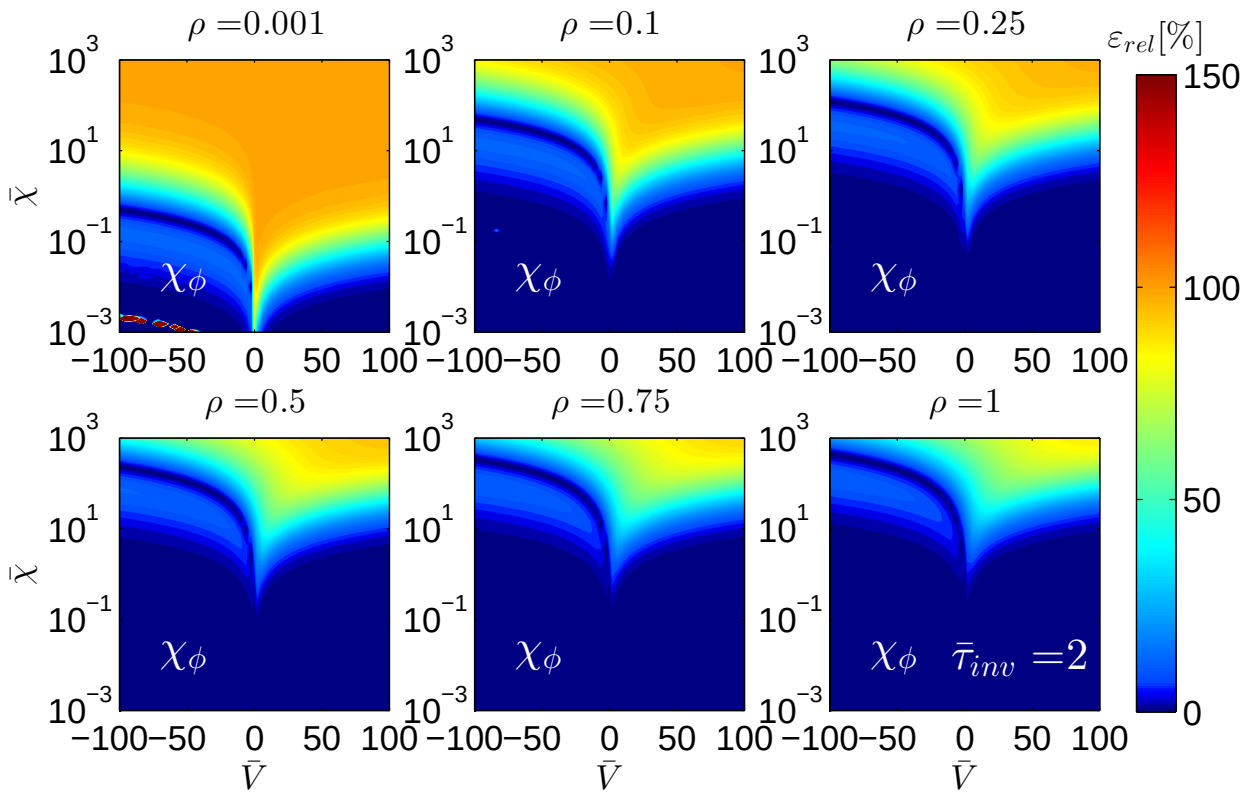

Figure 4: The relative errors of the χ_ϕ estimates as function of $\bar{\chi} = \chi/\omega$, $\bar{V}$ and ρ. The errors are based on a cylindrical geometry using an infinite domain boundary condition where χ, V, and $\bar{\tau}_{inv} = 2$ are independent of ρ. The heat waves travel outwards. The darkest blue represents $\varepsilon_{rel} < 1\%$ and the darkest red represents all $\varepsilon_{rel} > 150\%$.

In general χ can be approximated well for large ρ as it than behaves more slab-like. On the other hand, for large $\bar{\chi}$ and small ρ the cylindrical effects are stronger, thus the errors are large. The effect of the damping coefficients is not shown here as it is rather small. The approximation χ_V can also be used when $\tau_{inv} = 0$ and performs well, but only for positive V. In the next section, it is discussed how to estimate the convectivity and damping and their common errors.

VII. ESTIMATING THE CONVECTIVITY AND DAMPING

In this section, the possibility of estimating the convectivity V and damping τ_{inv} in a semi-infinite cylindrical domain is investigated based on the slab-geometry estimates V_ϕ and τ_ϕ. Then, the effect of model errors arising from idealized assumptions are studied in a

slab-geometry to distinguish between errors arising from the idealized assumptions and the cylindrical geometry.

A. Estimation of V and τ_{inv} in a semi-infinite cylindrical geometry

The only possibility to estimate χ in a cylindrical geometry under the influence of V and τ_{inv} presented here is by using χ_ϕ in (41). The accompanying V_ϕ in (42) and τ_ϕ in (44) give the slab estimates V_s and τ_{invs} and not the cylindrical V and τ_{inv}. The quality of these estimates using V_s and τ_{invs} is investigated on the basis of a semi-infinite cylindrical geometry and is presented in Fig. 5.

The slab approximation V_ϕ still gives a good estimate of the cylindrical geometry, because the damping takes part of the model errors into account (see (11)). However, this also means that the estimates of τ_{inv} in a cylindrical geometry are poorly approximated by τ_ϕ (not shown here). On the other hand, it is also possible to compensate for the model errors based on (11), i.e.

$$V_\phi^{comp} = V_\phi - \frac{\chi_\phi}{\rho}, \text{ and } \tau_\phi^{comp} = \tau_\phi + \frac{2}{3}\frac{V_\phi}{\rho}. \tag{48}$$

The compensated V_ϕ^{comp} improves the estimate of V in some regions, but decreases it in other regions. However, this can be understood by comparing V_ϕ^{comp} to χ in Fig. 4. The region where V_ϕ^{comp} approximates V well is almost an exact copy of the region where χ_ϕ approximates χ well in Fig. 4. In (48), it also becomes clear that there is a clear relationship between the chosen base geometry (slab, cylindrical) and the variation of the transport coefficients. If one allows, the transport coefficients V_s and τ_s to be spatial dependent then it is possible to transform a cylindrical geometry into a slab geometry.

The damping can only be estimated by the use of τ_ϕ^{comp} in a limited region. One might expect that by replacing V_ϕ by V_ϕ^{comp} to calculate τ_ϕ^{comp} might increase the approximation region, but the differences are rather small.

It is clear that the slab approximations with or without compensation can approximate the convectivity and damping in a semi-infinite cylindrical geometry with constant parameters in certain parameter ranges of $\bar{\chi}$, $\bar{V}$, $\bar{\tau}_{inv}$, and ρ. However, in reality the profiles can vary spatially and a different boundary condition is present than the infinite domain. The effect of these varying profiles and different boundary conditions on the estimates of χ, V, and τ_{inv} is investigated next.

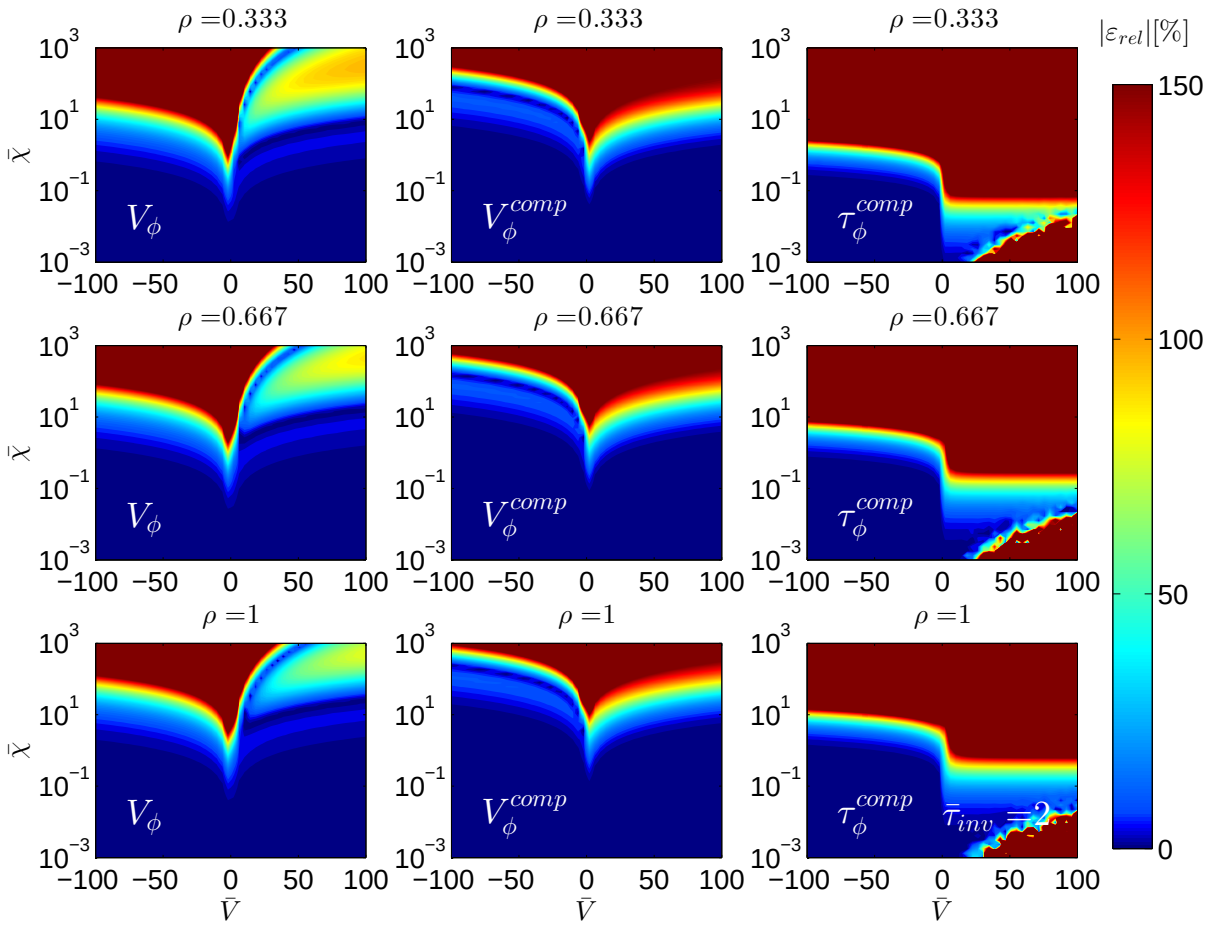

Figure 5: The relative error of the estimates of V and τ_{inv} using the approximations V_ϕ, V_ϕ^{comp}, and τ_ϕ^{comp} for a large range of $\bar{\chi}$, $\bar{V}$, and ρ. This comparison is based on a cylindrical geometry using an infinite domain, where the heat waves travel outwards. The darkest blue represents $\varepsilon_{rel} < 1\%$ and the darkest red represents all $\varepsilon_{rel} > 150\%$.

B. The effect of boundary conditions and radial dependent profiles

Here, the errors originating from (varying) spatial dependent profiles and boundary conditions are studied. It has been shown that using slab geometry approximations to estimate the transport coefficients in a cylindrical geometry also introduces errors. Therefore, a slab-geometry simulation is used here to distinguish between errors originating from varying profiles/boundary conditions and cylindrical geometry. Although only the errors for (41), (42), and (44) are shown, these errors occur for all approximations presented in this paper, including the ones from the literature, as they are based on the same assumptions.

The choice of an infinite domain description allows the derivation of explicit equations, which is an important advantage over other choices of the boundary conditions. However, the disadvantages are generally not so clear, but should also be considered: 1) it is assumed that the parameters are independent of ρ from $[\rho_i, \infty)$, so even variations far from the used A'/A and ϕ' will introduce an error on the estimated diffusivity even if it is locally constant in space and; 2) there is a difference between the modeled and the real boundary, i.e., estimates close to the real boundary will show a significant bias (errors). This was already shown in [39] using analytic expansions.

The introduced bias due to mismodeling is partly suppressed in practice. This is because (10) acts as a low-pass filter, suppressing high-frequency errors more strongly than low-frequency information. The amount of suppression also depends on the distance to the boundary, on the variation of the parameters, and on the distance of this variation to the location ρ. However, as τ_{inv} and V are influenced by low-frequency information, they are affected more strongly by these errors, making it often impossible to find the correct τ_{inv} and V.

These effects can be shown through an example. Therefore, the heat-transport model in slab (10) is discretized using finite difference and simulated with boundary conditions $\partial T/\partial\rho\,(\rho = 0) = 0$ and $T\,(\rho = 2.2) = 0$ with a (point) source term at $\rho = 0.0025$. Heat waves are studied traveling towards the edge. The choice for slab-geometry and heat waves towards the edge is made, because under these assumptions χ_ϕ, V_ϕ, and τ_ϕ, using (41), (42), and (44), exactly determine χ, V_s, and τ_{invs} such that only the effect of varying profiles and boundary conditions influence the result. A finite difference simulation is used with 2000 measurement (spatial grid) points, which are equidistant with $\Delta\rho = 0.001$. The phase and amplitude as function of ρ are calculated from this finite difference simulation. The corresponding A'/A and ϕ' are calculated using (27), because this is the correct way to calculate A'/A and ϕ' in the case of slab-geometry. In addition, as the distance between two points $\Delta\rho$ is very small, the errors in A'/A and ϕ' are negligible. The dimensionless radius ρ has been extended here to two to more clearly show the errors originating from varying profiles and boundary conditions. The result is shown in Fig. 6, where a varying profile of χ and V_s in terms of steps are shown. It is clear that the estimates of χ_ϕ feel the step in $\chi\,(\rho)$ before it occurs, which is, as explained, a direct consequence of choosing infinite domains. However, interestingly at the step in $\chi\,(\rho)$ $(\rho = 0.5)$ the estimates χ_ϕ and V_ϕ are close to

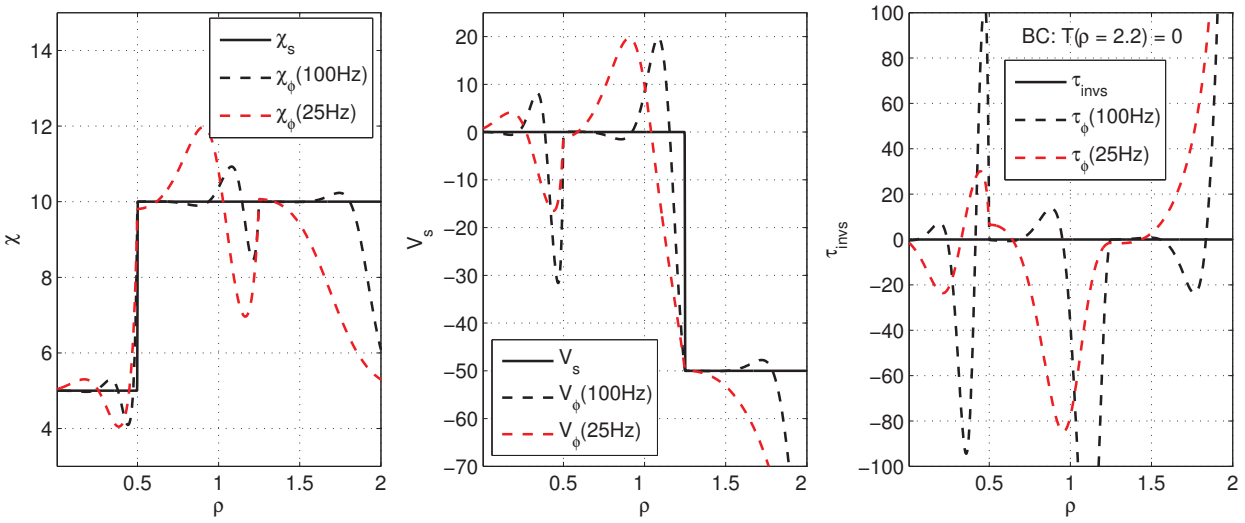

Figure 6: Comparison between two estimated profiles with a step in the $\chi(\rho)$ profile at $\rho = 0.5$ and in the $V_s(\rho)$ at $\rho = 1.25$. In addition, following boundary condition $T(\rho = 2.2) = 0$ is applied. Two estimates of χ, V_s, and τ_{invs} expressed as χ_ϕ, V_ϕ, and τ_ϕ are presented for the combination 25 Hz and 50 Hz, *and* 100 Hz and 200 Hz, i.e., the first two harmonics are used.

the true values. The small difference at the step in $\chi(\rho)$ at $\rho = 0.5$ is caused by the step in $V_s(\rho)$ at $\rho = 1.25$, which influences the estimates at $\rho = 0.5$. The same phenomenon can be observed at the step in $V_s(\rho)$ where both the estimates χ_ϕ and V_ϕ are exact. Due to (17) the estimates are insensitive to what happens before $\phi_1 = \phi(\rho_1)$. However, in principle, they are sensitive to what happens at $\rho > \rho_1$, hence τ_{inv} is not exact at the steps. The estimates that come close to the boundary condition will also show errors, as was already discussed in [39].

A different aspect is the magnitude of variation in the estimates due to variations in the profiles and boundary conditions. Therefore, it is important to consider the y-scales in Fig. 6. The variations in the profiles influence χ to a lesser extend, but are disastrous for the estimates of V_s and τ_{invs}. Moreover, a step in $\chi(\rho)$ has a large influence on the estimates V_ϕ and τ_ϕ, but a step in $V_s(\rho)$ and $\tau_{invs}(\rho)$ (not shown here) influences χ_ϕ to a lesser extent. Note, that the step in $V_s(\rho)$ is 10 times larger than the step in $\chi(\rho)$.

The errors introduced by the boundary errors show a similar behavior, which are significantly larger for V_ϕ and τ_ϕ. The main reason why the errors are significantly larger for τ_ϕ and to a lesser extent V_ϕ is that errors propagate further at low frequencies. Both, $V_s(\rho)$

and $\tau_{invs}(\rho)$ are only important at low frequencies, see (14). This also explains why the estimate of χ using 25 Hz show larger errors than the estimate based on 100 Hz.

We refrain here from making statements about direction and absolute values of errors as this depends on too many factors such as the boundary conditions, the absolute values and the variation of profiles, frequency, how A'/A and ϕ' are approximated, etc. Therefore, only the qualitative behavior is shown, which also led us to the conclusion that V_s and τ_{invs} will be very difficult to study in practice using infinite domains. This also holds for the estimates of the cylindrical V and τ_{inv}. On the other hand, a step in a profile is also the most extreme case and different boundary conditions probably hold. This means that it is not always impossible to estimate V_s and τ_{invs} or V and τ_{inv} in practice, but great care should be taken and different approximation methods for V and τ_{inv} may be necessary.

The argument could be made that these errors are suppressed by increasing the frequency of the perturbation source, but that will lead to noisy measurements. A better solution is to use implicit methods, which allow the use of much more complex models without many of the problems encountered by infinite domains. In that case the approximations presented in this paper form a tool for finding starting values for such implicit methods and to have a rough idea of the values of $\chi(\rho)$. However, this is not the subject of this paper.

VIII. SUMMARY AND DISCUSSION PART 1

In this paper, the problem of determining the thermal diffusion coefficient from electron temperature measurements during power modulation experiments has been revisited. A number of new approximations have been introduced to estimate χ, V, and τ_{inv} directly from A'/A and ϕ' for different combinations of χ, V, and τ_{inv}. The approximations are based on infinite slab domains using common assumptions. To gain an understanding of how ϕ and A are related to A'/A and ϕ', on which the approximations are based, the notion of transfer functions is introduced. This makes the relationship between ϕ' and ϕ explicit. The study of this relationship also shows that the dependency of ρ is contained in A' and ϕ' and as such depends on how A' and ϕ' are calculated.

The main result is the approximation of χ, under the influence of V and τ, based on the phases of two harmonics. Hence, this new approximation is less sensitive to calibration errors. The new approximation extends the region in which χ can be approximated compared to

the well known relationship in [9] for cylindrical geometry even if $V = 0$. However, it should be noted that unlike the relationship in [9], the new approximation does not take density gradients into account and is based on the phase of two harmonics instead of amplitude and phase of one harmonic. This approximation performs well in a large region when convectivity is present for which no direct expression is currently available. Here, the use of two harmonics cannot be seen as a deficit as always at least two harmonics will be necessary.

Also the use of infinite domains necessary to arrive at explicit approximations are discussed. The infinite domain assumption introduces errors, which are related to varying profiles and boundary conditions. Moreover, these errors influence the convectivity and damping significantly, making the estimated V and τ_{inv} often erroneous. On the other hand, it is important to still estimate V and τ_{inv} as they can be used to select the proper approximation and to verify if the estimates of χ in the presence of V and τ_{inv} are correct. This will be explained in Part 2, where a number of new approximations are derived. The results in Part 2 are based directly on a semi-infinite cylindrical domain.

IX. ACKNOWLEDGMENTS

The authors want to acknowledge Dr. Jonathan Citrin and Dr. Tatsuya Kobayashi for the discussion on turbulent transport and zonal flows.

The first author is an international research fellow of the Japan Society for the Promotion of Science and hence wishes to express his gratitude to the JSPS for making this research possible. This project has received funding from the European Union's Horizon 2020 research and innovation programme under grant agreement number 633053. The views and opinions expressed herein do not necessarily reflect those of the European Commission. This work is also supported by NWO-RFBR Centre-of-Excellence on Fusion Physics and Technology (Grant nr. 047.018.002).

[1] N. J. Lopes Cardozo, "Perturbative transport studies in fusion plasmas," *Plasma Phys. Control. Fusion*, vol. 37, p. 799, 1995.

[2] S. P. Eury, E. Harauchamps, X. Zou, and G. Giruzzi, "Exact solutions of the diffusion-convection equation in cylindrical geometry," *Physics of Plasmas*, vol. 12, p. 102511, 2005.

[3] G. M. D. Hogeweij, J. O'Rourke, and A. C. C. Sips, "Evidence of coupling of thermal and particle transport from heat and density pulse measurements in JET," *Plasma Phys. Control. Fusion*, vol. 33, no. 3, p. 189, 1991.

[4] G. Jahns, M. Soler, B. Waddell, J. Callen, and H. Hicks, "Internal disruptions in tokamaks," *Nuclear Fusion*, vol. 18, no. 5, p. 609, 1978.

[5] M. Soler and J. Callen, "On measuring the electron heat diffusion coefficient in a tokamak from sawtooth oscillation observations," *Nuclear Fusion*, vol. 19, no. 6, p. 703, 1979.

[6] J. D. Callen and G. L. Jahns, "Experimental measurement of electron heat diffusivity in a tokamak," *Phys. Rev. Lett.*, vol. 38, pp. 491–494, Feb 1977.

[7] N. L. Cardozo, B. Tubbing, F. Tibone, and A. Taroni, "Heat pulse propagation: Diffusive models checked against full transport calculations," *Nuclear Fusion*, vol. 28, no. 7, p. 1173, 1988.

[8] E. Fredrickson, J. Callen, K. McGuire, J. Bell, R. Colchin, P. Efthimion *et al.*, "Heat pulse propagation studies in TFTR," *Nuclear Fusion*, vol. 26, no. 7, p. 849, 1986.

[9] A. Jacchia, P. Mantica, F. De Luca, and G. Gorini, "Determination of diffusive and nondiffusive transport in modulation experiments in plasmas," *Physics of Fluids B*, vol. 3, no. 11, pp. 3033–3040, 1991.

[10] F. Ryter, R. Dux, P. Mantica, and T. Tala, "Perturbative studies of transport phenomena in fusion devices," *Plasma Phys. Control. Fusion*, vol. 52, p. 124043, 2010.

[11] S. Inagaki, H. Takenaga, K. Ida, A. Isayama, N. Tamura, T. Takizuka, T. Shimozuma, Y. Kamada, S. Kubo, Y. Miura *et al.*, "Comparison of transient electron heat transport in LHD helical and JT-60U tokamak plasmas," *Nuclear Fusion*, vol. 46, no. 1, p. 133, 2006.

[12] J. DeBoo, C. Petty, A. White, K. Burrell, E. Doyle, J. Hillesheim, C. Holland, G. McKee, T. Rhodes, L. Schmitz *et al.*, "Electron profile stiffness and critical gradient studies," *Physics of Plasmas*, vol. 19, p. 082518, 2012.

[13] P. Mantica and F. Ryter, "Perturbative studies of turbulent transport in fusion plasmas," *Comptes Rendus Physique*, vol. 7, no. 6, pp. 634–649, 2006.

[14] T. C. Luce, C. C. Petty, and J. C. M. de Haas, "Inward energy transport in tokamak plasmas," *Phys. Rev. Lett.*, vol. 68, pp. 52–55, Jan 1992. [Online]. Available: http://link.aps.org/doi/10.1103/PhysRevLett.68.52

[15] K. W. Gentle, "Dependence of heat pulse propagation on transport mechanisms: Consequences

of nonconstant transport coefficients," *Physics of Fluids*, vol. 31, p. 1105, 1988.

[16] J. P. Freidberg, *Plasma Physics and Fusion Energy*. Cambridge University Press, 2007.

[17] J. Wesson, *Tokamaks*. OUP Oxford, 2011, vol. 149.

[18] P. H. Diamond, S.-I. Itoh, K. Itoh, and T. S. Hahm, "Zonal flows in plasma – a review," *Plasma Physics and Controlled Fusion*, vol. 47, no. 5, p. R35, 2005. [Online]. Available: http://stacks.iop.org/0741-3335/47/i=5/a=R01

[19] A. Fujisawa, "A review of zonal flow experiments," *Nuclear Fusion*, vol. 49, no. 1, p. 013001, 2009. [Online]. Available: http://stacks.iop.org/0029-5515/49/i=1/a=013001

[20] P. H. Diamond, M. N. Rosenbluth, E. Sanchez, C. Hidalgo, B. Van Milligen, T. Estrada, B. Brañas, M. Hirsch, H. J. Hartfuss, and B. A. Carreras, "In search of the elusive zonal flow using cross-bicoherence analysis," *Phys. Rev. Lett.*, vol. 84, pp. 4842–4845, May 2000. [Online]. Available: http://link.aps.org/doi/10.1103/PhysRevLett.84.4842

[21] L. Chen, Z. Lin, and R. White, "Excitation of zonal flow by drift waves in toroidal plasmas," *Physics of Plasmas*, vol. 7, no. 8, pp. 3129–3132, 2000.

[22] H. Bateman and A. Erdelyi, *Higher transcendental functions*, A. Erdelyi, Ed. Mcgraw-Hill, New York, 1953.

[23] A. Cuyt, V. B. Petersen, B. Verdonk, H. Waadeland, and W. B. Jones, *Handbook of continued fractions for special functions*. Springer Netherlands, 2008.

[24] W. B. Jones and W. T. C. Fractions, *Analytic Theory and Applications*, ser. Encyclopedia of Mathematics and its Applications. Addison-Wesley Publishing Company, London, 1980, vol. 11.

[25] A. Erdélyi, *Asymptotic expansions*. Courier Dover Publications, NY, 1956.

[26] L. Slater, *Confluent hypergeometric functions*. Cambridge University Press, Cambridge, 1960.

[27] J. C. M. De Haas, J. O'Rourke, A. C. C. Sips, and N. J. Lopes Cardozo, "Interpretation of heat and density pulse measurements in jet in terms of coupled transport," *Nuclear Fusion*, vol. 31, p. 1261, 1991.

[28] C. M. Bishop and J. W. Connor, "Heat-pulse propagation in tokamaks and the role of density perturbations," *Plasma Phys. Control. Fusion*, vol. 32, no. 3, p. 203, 1990.

[29] R. F. Curtain and H. J. Zwart, *An Introduction to Infinite-Dimensional Linear Systems Theory*. Springer-Verlag New York, 1995, vol. 21.

[30] A. D. Polyanin and V. F. Zaitsev, *Handbook of Exact Solutions for Ordinary Differential*

Equations. Chapman & Hall/CRC, London, 2003, vol. 2.

[31] T. Dudok de Wit, B. P. Duval, B. Joye, and J. B. Lister, "Measurement of hydrogen transport in deuterium discharges using the dynamic response of the effective mass," *Nuclear Fusion*, vol. 31, p. 359, 1991.

[32] J. M. Moret, T. Dudok de Wit, B. Joye, and J. B. Lister, "Investigation of plasma transport processes using the dynamical response of soft x-ray emission," *Nuclear Fusion*, vol. 33, no. 8, pp. 1185–1200, 1993, cited By (since 1996): 8.

[33] G. Witvoet, M. de Baar, E. Westerhof, M. Steinbuch, and N. Doelman, "Systematic design of a sawtooth period feedback controller using a kadomtsev-porcelli sawtooth model," *Nuclear Fusion*, vol. 51, no. 7, p. 073024, 2011. [Online]. Available: http://stacks.iop.org/0029-5515/51/i=7/a=073024

[34] R. Pintelon and J. Schoukens, *System Identification: A Frequency Domain Approach*. Wiley-IEEE Press, Hoboken (NJ), 2012.

[35] L. Ljung, *System identification*. Wiley Online Library, 1999.

[36] R. F. Curtain and K. Morris, "Transfer functions of distributed parameter systems: A tutorial," *Automatica*, vol. 45, no. 5, pp. 1101–1116, 2009.

[37] M. van Berkel, H. J. Zwart, G. M. D. Hogeweij, G. Vandersteen, H. van den Brand, M. R. de Baar, and the ASDEX Upgrade Team, "Estimation of the thermal diffusion coefficient in fusion plasmas taking frequency measurement uncertainties into account," *Plasma Phys. Control. Fusion*, vol. 56, p. 105004., 2014.

[38] P. Mantica, F. Ryter, C. Capuano, H. U. Fahrbach, F. Leuterer, W. Suttrop, J. Weiland, and ASDEX-Upgrade Team, "Investigation of electron heat pinch in ASDEX-Upgrade," *Plasma Phys. Control. Fusion*, vol. 48, no. 3, p. 385, 2006.

[39] W. Goedheer, "Inference of electron heat conductivity from the propagation of a temperature perturbation in the outer confinement region of a tokamak," *Nuclear Fusion*, vol. 26, no. 8, p. 1043, 1986.